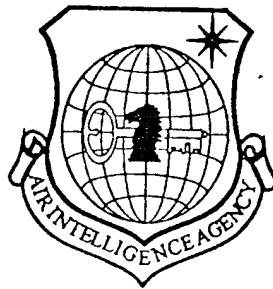


NATIONAL AIR INTELLIGENCE CENTER



USE OF PRECRACKING METHOD TO INVESTIGATE THE FRACTURE
TOUGHNESS (K_{IC}) OF CERAMIC MATERIALS

by

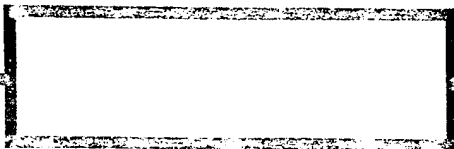
Guangxin Li, Zhihao Jin, et al.



DTIC QUALITY INSPECTED 5

19950512 048

Approved for public release;
Distribution unlimited.



HUMAN TRANSLATION

NAIC-ID(RS)T-0650-94 14 April 1995

MICROFICHE NR: 95000212

USE OF PRECRACKING METHOD TO INVESTIGATE THE FRACTURE
TOUGHNESS (K_{IC}) OF CERAMIC MATERIALS

By: Guangxin Li, Zhihao Jin, et al.

English pages: 14

Source: Xian Jiaotong Daxue Xuebao, Vol. 27, Nr. 3,
June 1993; pp. 19-24

Country of origin: China

Translated by: SCITRAN
F33657-84-D-0165

Requester: NAIC/TATV/Robert M. Dunco

Approved for public release; Distribution unlimited.

THIS TRANSLATION IS A RENDITION OF THE ORIGINAL FOREIGN TEXT WITHOUT ANY ANALYTICAL OR EDITORIAL COMMENT STATEMENTS OR THEORIES ADVOCATED OR IMPLIED ARE THOSE OF THE SOURCE AND DO NOT NECESSARILY REFLECT THE POSITION OR OPINION OF THE NATIONAL AIR INTELLIGENCE CENTER.

PREPARED BY:

TRANSLATION SERVICES
NATIONAL AIR INTELLIGENCE CENTER
WPAFB, OHIO

GRAPHICS DISCLAIMER

All figures, graphics, tables, equations, etc. merged into this translation were extracted from the best quality copy available.

Accession For	
NTIS CRA&I	<input checked="" type="checkbox"/>
DTIC TAB	<input type="checkbox"/>
Unannounced	<input type="checkbox"/>
Justification _____	
By _____	
Distribution /	
Availability Codes	
Dist	Avail and/or Special
A-1	

USE OF PRECRACKING METHOD TO INVESTIGATE
THE FRACTURE TOUGHNESS (K_{IC}) OF CERAMIC MATERIALS¹

/19*

Guangxin Li, Zhihao Jin, Jiqiang Gao and Jianfeng Yang²

Abstract

From TZP ceramic materials, precracked ceramic samples were prepared, to explore the precracking method in measuring K_{IC} and its influencing factors, and thus a suggestion was made possible on a better method to control the spreading of any fracture; analysis and discussion were made on whether loading speed, phase transformation, residual stresses and other influencing factors could affect K_{IC} of the fractured samples, thus to perfect this method in improving its use in manufacturing applications.

Keywords: Ceramics, Crack, fracture-toughness
Chinese Library Materials Classification Method,
Classification Number: TB302.3

0. Introduction

For fracture toughness K_{IC} , which is a quality indicator of material science, there are a lot of testing methods available now in the ceramic area. For instance, single edge breaching method (SENB), Injury-pressurizing method (IM), Double twisting method (DT), etc. All these methods are so different, the measured data have tremendous discrepancies, and it is very difficult to compare the

* Numbers in margins indicate foreign pagination.
Commas in numbers indicate decimals.

¹ The data received: November 1, 1991.

² Department of Material Engineering.

results of the measurements from all these different experimental methods [1]; and there is no way one can compare them with the K_{IC} data from metallic materials and other materials. Consequently, it is a necessary condition in studying fracture toughness of materials to find a testing method which can incorporate all these kinds of materials in a unified way. This paper suggests the single-edge cracking method to test KIC of ceramic materials and it is a method transplanted from a metal-testing technique to be used to test ceramic materials here, a precracking technique to prepare a single-edge penetrating prefractures on the ceramic samples and then by use of the 3-point-bending loading method to test KIC of the ceramic materials, achieving a meeting between the ceramic KIC testing and the metallic KIC testing method.

1. Materials and Sample Preparation

1.1 The experimental materials

The materials used in this paper was the partially stabilized ZrO_2 (containing 3 mol% Y_2O_3), namely TZP, in a powdery state with the original corpuscularity $\ll 0.1 \mu m$, going through a particle-formation, shape-formation and fusing-together, and their physical property indicators are as follows: Porousness $P_a = 0.6\%$, body density: $D_o = 5.98 \text{ gm/cm}^3$, Crystalline degree $\leq 0.7 \mu m$, bending strength at ordinary temperatures: $\sigma_f = 700 \text{ MPa}$, the sample magnitude for the fracture toughness (K_{IC}) was 3mm x 4mm x 40mm, and the computation formula for the 3-point-bending loading is as follows:

$$K_{IC} = \frac{P_{max} S}{B W^{3/2}} \left[2.9 \left(\frac{a}{w} \right)^{1/2} - 4.6 \left(\frac{a}{w} \right)^{3/2} + 21.8 \left(\frac{a}{w} \right)^{5/2} - 37.6 \left(\frac{a}{w} \right)^{7/2} + 38.7 \left(\frac{a}{w} \right)^{9/2} \right] \quad (1)$$

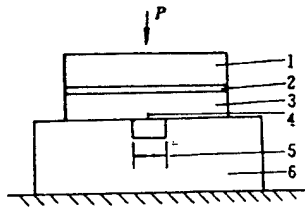
where P_{max} is the maximum load during the time when the fracture was prepared, S is the pacing step-distance, B the sample thickness, W is the sample height and a is the length of the crack.

1.2 Precracking and Analysis

To prepare the K_{IC} sample, first one has to pick the location for the precracked fracture by pressuring there to create the injury, and then apply a bending loading on the sample to spread out the fracture to a certain desired length [1]. The precracking job was done on a HV-120 type strength-testing machine and Instron 1195 electric power pulling experimental apparatus.

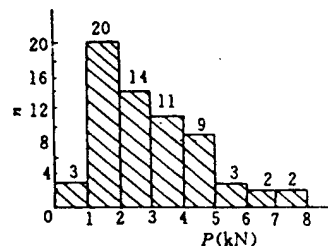
For the diagram of the uniform distribution of load applied to the precracked location, one can see it in Fig.1.

Fig. 1 The sketch of the even distribution of the bending load



Key: 1 - Top pressuring kind; 2 - Soft material; 3 - The sample; 4 - The crack; 5 - Concave vessel; 6 - Supporting frame

Fig. 2 Statistical Distribution of the load applied at equal bending distances on the precracked fracture



Due to the effects of the elastic profile of the material and its pressure-resisting strength, the compressed area as well as both faces of the sample were not always receiving perfectly parallel forces and thus the crack frequently spread out crookedly [2]. The experimental results make it clear that : By placing a layer of soft material between the top pressure load and the sample, one can greatly reduce the required total load which could spread the fracture. Fig. 2 is to show the statistical distribution of the load imposed on the fracture under the condition of providing a layer of soft material. From the figure one can see that among the precracked samples, those receiving less than 5 kN of loads occupied 89 % while the maximum load was 8 kN; that is, it was only 1/4 - 1/6 times of the load if the soft material had not been added [2], and thus it could effectively prevent the crooked development of the fracture.

2. Analyzing and discussing the experimental method

2.1 The condition for the cracking dynamics

The planar strain and the condition of a small scale pliability are the preconditions for preparing the K_{IC} material. Metallic material has a better plasticity, and there is an intimate relationship between its critical stress factor (K) and the sample thickness (B), fracture length (a) and the width of toughened band (w-a). Metallic material demands the size of the K_{IC} sample to exceed the limits set up by the following expression:

$$\left. \begin{array}{l} B \\ a \\ w-a \end{array} \right\} \geq C(K_{IC}/\sigma_t)^2$$

where C is the coefficient (for metallic materials, usually $C = 2.5$).

The property of a ceramic material is hard but brittle, having the lowest plasticity, as well as a very low ratio of K_{IC}/σ_f [3,4]. Usually $K_{IC}/\sigma_f < 0.02$, which can always satisfy the conditions of Eqn.(1); that is, if one considers the inhomogeneity in the structure of ceramic materials the cross-section of a sample has enough area to establish structural characteristics (in using a 3mm x 4mm x 40mm sample), and $C_{ceramic}$ is larger than C_{metal} by a factor of 4. Consequently one can see that from the analyses with the linear elastic theory, the measured values of ceramic K_{IC} must be more able to reflect the nature of the material than in the case of metallic materials. Table 1 shows the effect of difference in lengths of the fractures on the measured values of K_{IC} .

From Table 1 one can see that although the length of a crack would change in quite a large scale, yet the change in the measured K_{IC} values was rather small, even lower than the fluctuation degree in the data from the equal fracture lengths. Such property greatly simplifies the preparation of cracks to a ceramic K_{IC} sample, even though the precracked lengths are allowed to be in a rather wide range.

Table 1 The measured K_{IC} values for various precracked lengths

1 编号	1	2	3	4	5	6	7	8
2 裂纹长度 a (mm)	3.091	3.375	3.209	2.651	1.307	1.045	1.578	1.180
a/w	0.784	0.840	0.844	0.717	0.355	0.279	0.422	0.310
K_{IC} (MPa \sqrt{m})	4.820	4.415	4.495	5.182	5.271	4.128	5.214	4.957
3 平均值	4.728			4.893				

4 注:表中试样均经人工时效去应力退火

Key: (1) Index numbers (2) Prefractured lengths
 (3) Average values (4) Note: All the samples in the table have been annealed of stresses with some artificial formulas

2.2 Critical Load

Plasticity of all the ceramic materials is extremely different, and furthermore it refuses to deviate from the linear elastic dynamic system easily, until the crack starts to spread. To simplify the experiment, this paper skipped the testing of the process for the crack to start to initiate some displacement, but the K_{IC} calculation proceeded by use of the maximum load at which the crack replaces the one which makes the spreading point unstable [5].

2.3 Loading speed

The measured K_{IC} values for various loading speeds can be seen in Fig.3. From Fig.3 one can see that if the loading speed is in the range between 0.5 mm/min and 5

mm/min, K_{IC} displays the maximum value, while for $V < 0.5$ mm/min K_{IC} grows with increasing V . For $V > 5$ mm/min, K_{IC} declines with increasing V .

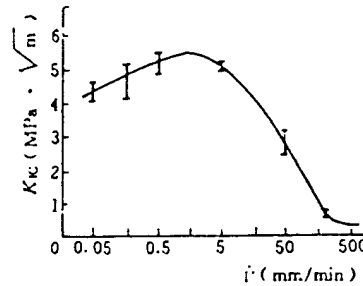


Fig. 3 The K_{IC} values for various different loading speeds

In Fig. 3, one of the reasons why K_{IC} follows the change of the loading speed could be related to the fact that the crack creates some kinds of subcritical expansion. At a low loading speed, K at the tip of the crack grows slowly, and when K reaches the critical K_{IC} , it lets the fracture create the condition for some subcritical expansion to appear.

The length of the crack in this experiment was the average of the precracked lengths of the measured fractures, observed with an optical microscope. Because in this experiment it is difficult to distinguish the subcritical expansion created by the fracture from any fracture opening created by some instability, it is still not possible to accurately measure the length of the fracture before instability sets in. Substituting the length of the precracked fracture for the fracture length which appeared when some instability started to create fractures could make the actual loading area ($w-a_1$) smaller than the calculated loading area ($w-a_0$), to make the calculated K_{IC} value too low. Besides, it also made a/w acquire errors.

Raising loading speed can shorten the time for K to reach K_{IC} , thus having the advantage of suppressing the process of subcritical spread. The study on the development of subcritical spreading process of the fracture under a double twisting state shows: When the spreading speed of fracture $V_c \geq 10^{-3}$ m/s, one can recognize the location of fracture which is in the state of some unstable spreading [6]. From Fig. 3 it is clear that in the 3-point-bending, the loading speed which corresponds to V_c , exists in the interval between 0.5 mm/min and 5 mm/min.

An even higher loading speed will greatly suppress K_{IC} , and this paper found that this has something to do with the material which resisted any motional loading, and at this time K_{IC} and strength (σ_f) agreed with the change of the loading speed.

2.4 Phase Transition increases toughness

The effect of getting tougher by phase transformation in TZP zirconium oxide depends on whether the rectangular phase can turn into some rhombic phase ($t \rightarrow m$), and such transformational process brings down the free energy of the system as follows:

$$\Delta G_{chem} \geq \Delta U_t - \Delta U_a \quad (3)$$

where ΔG_{chem} is the free energy difference between the m-phase and t-phase; ΔU_t is the change in the elastic potential energy; ΔU_a is the energy provided by some external stress to stimulate the phase-transition.

If the external stress can bring about $\Delta U_a \geq \Delta U_t - \Delta G_{\text{chem}}$, then the phase-transition can occur; that is, in the vicinity of the fracture tips of the precracked K_{IC} sample, the condition to effect the $t \rightarrow m$ transformation is for the stress or the stress field to exceed a certain critical value ($\Delta U_t - \Delta G_{\text{chem}}$), that can be shown as follows:

$$K_i \geq K_c \quad (4)$$

where K_i is the intensity factor of the stress at the fracture tip at a certain time, and K_c the critical value for the corresponding intensity factor of the stress to induce $t \rightarrow m$ the phase transition ($K_c = \Delta U_t - \Delta G_{\text{chem}}$).

The speed of crack propagation $V = A K^*$ implies the existence of a certain crack-propagation value:

$$V_c = AK_c^2 \quad (5)$$

Now if $V > V_c$, at the tip of the fracture the $t \rightarrow m$ phase-transition can occur, while if $V < V_c$, the crack will spread out; that is, the stress field at the tip of the crack is not sufficient to induce a phase-transition and thus the toughening-up via a phase-transition cannot occur.

To summarize the analyses of Fig. 3, at a slow loading because the amount of $t \rightarrow m$ phase-transition is small, the toughening-up effect does not show, and the contribution to K_{IC} is small; as the loading speed is raised, the amount of phase transition gradually intensifies, the appearance of the toughening-up effect increases and K_{IC} is enhanced. This is again one of the reasons how the loading speed can affect K_{IC} .

2.5 Residual Stress

The residual stress at the tip of a crack is mainly from 2 directions, one: When the precracked fracture is eliminated by some external force, the coarse rupture at the surface cannot sufficiently close up, and the convex spots making contact with one another perpetuate a constant amount of fractures, to create a residual stress field to preserve the tips of the crack; second: is the reversibility of the $t \rightarrow m$ phase-transition in TZP ceramic materials; after the external force is eliminated, the reverse phase transition process $m \rightarrow t$ occurs, to create a new stress field at the tip of the newly built crack. These 2 kinds of residual stresses interact, it affects not only the material structure, but also the way with which loading is made, to create rather large adaptable adjustments, such as the shape of the crack, direction of propagation, degree of surface coarseness at the crack, and the distribution of the t-phase, etc. This is a very complicated and difficult research subject. As a study of the experimental methods, what is relevant here is the effect of residual stress on the experimental results. Theoretically speaking, when a crack starts to propagate, it could lower the residual stress and for $V = 0$ the residual stress reaches the lowest limit, but a prescribed method can achieve this objective. The study of the effect of residual stress on K_{IC} by a natural prescription method clarifies that for a sufficient long duration, a natural prescription can raise the K_{IC} value a little higher [1]. However, a natural prescription takes a long time to do the job and thus it cannot be used in an actual experiment; consequently it makes more sense to let an artificial prescription replace a natural prescription.

In this paper the artificial prescription and the experimental method are as follows: First, separately measure the rupture lengths of the two sides of the sample and then heat the sample, cool it down in an insulated oven, then measure again the rupture lengths; the difference will be the spread of the crack. Measuring the rupture lengths was done by a 400-optic microscope. For the effect of any artificial prescription on the ruptured length and K_{IC} , one may refer to Table 2 and Table 3.

Table 2 and Table 3 show that an artificial prescription can increase the length of a rupture, the measured K_{IC} value also goes up accordingly, and K_{IC} due to an artificial prescription is larger than K_{IC} due to a natural prescription. This explains that any prescription can dissipate the stress field at the tip of a crack. However, the spread of rupture does not seem to have any bearing on the temperature of heating and heat-preserving duration but has a lot to do with the adaptability of residual stresses.

Table 2 The effect of different heating temperatures and warmth-preserving durations on the ruptured lengths

① 编号	② 原始裂纹长度(mm)		⑤ 加热温度 (°C)	⑥ 保温时间 (h)	⑦ 终了裂纹长度(mm)		⑧ 裂纹扩展量(mm)	
	③ 左侧	④ 右侧			③ 左侧	④ 右侧	③ 左侧	④ 右侧
1	1.590	1.313	50	8	1.578	1.311	-0.012	-0.002
2	0.840	0.890	50	6	0.930	1.211	+0.090	+0.321
3	0.892	1.039	50	4	1.098	0.995	+0.206	-0.004
4	1.286	1.201	50	4	1.320	1.300	+0.034	+0.099
5	1.751	1.711	100	8	1.764	1.807	+0.007	+0.096
6	2.091	1.932	100	6	2.387	2.169	+0.297	+0.237

(续表 2) ⑨

① 编号	② 原始裂纹长度(mm)		⑤ 加热温度 (°C)	⑥ 保温时间 (h)	⑦ 终了裂纹长度(mm)		⑧ 裂纹扩展量(mm)	
	③ 左侧	④ 右侧			③ 左侧	④ 右侧	③ 左侧	④ 右侧
7	2.430	2.515	100	2	2.427	2.531	+0.003	+0.016
8	1.560	1.402	100	1	1.436	1.429	-0.124	+0.027
9	2.835	2.850	150	3	3.173	3.000	+0.338	+0.150
10	2.912	3.251	150	4	2.820	3.493	-0.092	+0.242
11	1.861	2.225	150	2	1.890	2.408	+0.032	+0.183
12	1.648	2.109	150	4	1.640	2.117	+0.008	+0.008

Key: (1) Index (2) Original length of fracture (mm)
 (3) Left side (4) right side (5) heating temperatures (°C)
 (6) Warmth-preservation duration (h) (7) length of fractures at the end (mm) (8) Spread of the fractures (mm)
 (9) Table 2 - continued

Table 3 Comparing K_{IC} -data after either an artificial prescription or a natural prescription

编号	裂纹长度(mm)	a/w	时效方式	时效时间	$K_{IC}(MPa \cdot \sqrt{m})$
1	2.47		自然时效	20d	4.0
2	2.66		自然时效	20d	4.3
3	2.28		自然时效	20d	3.7
4	1.05		自然时效	150d	4.5
5	0.80		自然时效	150d	3.8
6	1.10		自然时效	150d	4.4
7	3.091	0.784	人工时效	150°C, 3h+200°C, 1h	4.8
8	3.375	0.840	人工时效	150°C, 3h+200°C, 1h	4.4
9	3.209	0.844	人工时效	150°C, 3h+200°C, 1h	4.5
10	2.651	0.717	人工时效	150°C, 3h+200°C, 1h	5.2
11	1.307	0.358	人工时效	100°C, 4h+150°C, 1h	5.3
12	1.045	0.279	人工时效	100°C, 4h+150°C, 1h	4.1
13	1.578	0.422	人工时效	100°C, 4h+150°C, 1h	5.2
14	1.180	0.310	人工时效	100°C, 4h+150°C, 1h	5.0

Key: (1) Index (2) Rupture lengths (mm)
 (3) Prescription methods (4) Prescription durations
 (5) Natural prescription (6) Artificial prescription

3. Conclusion

(1) The method of precracking ceramic materials is feasible, if one places a layer of some soft material between the top pressuring load and the sample so that it can greatly reduce the required loading and thus avoid the bending phenomenon of the fracture.

(2) The loading speed V has a definite effect on the measured K_{IC} in this precracking experiment. If V is smaller (< 0.5 mm/min), as V increases, K_{IC} grows; if V is bigger (> 5 mm/min), as V increases, K_{IC} declines; if speed is within the range between 0.5 mm/min $< V < 5$ mm/min, K_{IC} reaches the maximum value.

(3) An artificial prescription can reduce the stress field at the tip of a rupture so as to enhance the K_{IC} value, and its effect is better than that of a natural prescription and thus has practical significance.

References

- 1 Li Guangxin. A new method for measuring fracture toughness in ceramics by single edge crack beam. In: APCS-91. China, 328~332
- 2 Lemaitre P. Comparison of the fracture toughness of alumina measured by three different methods. J Mat Sci, 1988(7): 772~774
- 3 金志浩. 工程陶瓷材料. 北京: 机械工业出版社, 1986
- 4 郭景坤. 陶瓷的脆性与增韧. 硅酸盐学报, 1987, 15(5): 385
- 5 张清纯. 陶瓷材料的力学性能. 北京: 科学出版社, 1987, 374
- 6 王健. $Y_2O_3-ZrO_2$ 陶瓷的相变增韧效应与亚临界裂纹扩展特性: [博士论文]. 西安: 西安交通大学, 1990

DISTRIBUTION LIST

DISTRIBUTION DIRECT TO RECIPIENT

<u>ORGANIZATION</u>	<u>MICROFICHE</u>
B085 DIA/RIS-2FI	1
C509 BALLOC509 BALLISTIC RES LAB	1
C510 R&T LABS/AVEADCOM	1
C513 ARRADCOM	1
C535 AVRADCOM/TSARCOM	1
C539 TRASANA	1
Q592 FSTC	4
Q619 MSIC REDSTONE	1
Q008 NTIC	1
Q043 AFMIC-IS	1
E051 HQ USAF/INET	1
E404 AEDC/DOF	1
E408 AFWL	1
E410 AFDIC/IN	1
E429 SD/IND	1
P005 DOE/ISA/DDI	1
P050 CIA/OCR/ADD/SD	2
1051 AFTT/LDE	1
P090 NSA/CDB	1
2206 FSL	1

Microfiche Nbr: FTD95C000212
NAIC-ID(RS)T-0650-94